Dynamics below the depinning transition of interacting dislocations moving over fields of obstacles

R. Li, R. C. Picu, J. Weiss

Dynamics below the depinning transition of interacting dislocations moving over fields of obstacles

R. Li,[1] R. C. Picu,[1,*] and J. Weiss[2]

[1]*Department of Mechanical, Aerospace and Nuclear Engineering, Rensselaer Polytechnic Institute, Troy, New York 12180, USA*

[2]*Laboratoire de Glaciologie et Geophysique de l'Environnement, CNRS, 54 rue Moliere, BP 96, 38402 St. Martin d'Heres Cedex, France*

(Received 17 February 2010; published 31 August 2010)

The transition from the behavior of a single dislocation interacting with a field of fixed obstacles to the collective motion of multiple dislocations is studied below the depinning transition (thermally activated glide). In absence of interactions, a truncated power law distribution of jump amplitudes (avalanches) with a diverging cutoff toward the critical point, and intermittency are observed. Interactions lead to a modification of the correlation length exponent below the critical point and to more pronounced intermittency, a dynamics more compatible to acoustic emission experimental data.

DOI: 10.1103/PhysRevE.82.022107 PACS number(s): 46.65.+g, 61.72.Ff

Plastic deformation of crystalline solids mediated by dislocations has long been viewed as a smooth and homogeneous "plastic flow." A fundamentally different picture emerged during the last several years [1], that of a complex intermittent phenomenon characterized by dislocation avalanches [2], time correlations [3], fractal patterns, and space-time coupling [4]. Experimental evidences came first from acoustic emission (AE) measurements performed on single crystals of various materials (ice, Cd, Zn, Cu) exhibiting power law distributions of AE amplitude A, a proxy of the strain increment ε carried by the avalanche, $P(A) \sim A^{-\tau_A} f(A/A_0)$ [5,6]. The exponent $\tau_A = 2.0 \pm 0.1$ was found to be independent of the applied stress, temperature, strain hardening, or the material [6]. Scaling cutoff toward large amplitudes, described by $f(A/A_0)$, has been observed as the result of a nontrivial finite-size effect [6]. This cutoff does not evolve with the applied stress or strain. The AE results were then confirmed by deformation tests on micropillars [7] and by microextensometry experiments on macroscopic samples [6].

These results suggest a critical behavior of the dislocation system. The simplest modeling framework of this problem is the behavior of a single dislocation interacting with a random array of immobile obstacles [8–10] where long-ranged interactions between dislocations are neglected. This is a special case of the depinning transition for disordered elastic manifolds [11], for which one expects a jerky motion of the dislocation line with a power law distribution of jump size, S (the area swept by the dislocation during a jump) $P(S) \sim S^{-\tau_S} f(S/S_0)$. In this case, for an infinitely large system, the cutoff S_0 diverges as $S_0 \sim |\tau - \tau_c|^{-\chi}$ when approaching the critical shear stress τ_c either from above or from below. Approaching the critical stress from below is possible if thermal activation is allowed. This small scale limit of the problem is however in contradiction with the collective dislocation dynamics mentioned above on two fundamental points: (i) criticality is only obtained at the critical point $\tau = \tau_c$, i.e., the cutoff S_0 depends on the applied stress, and (ii) the exponent τ_S inferred from rough arguments or more sophisticated analyses is much lower than $\tau_A = 2$, the exponent measured in AE experiments. The depinning transition of a large array of interacting rigid dislocations was studied by Moretti *et al.* [12] above the critical stress for depinning (no thermal activation). They concluded that in terms of depinning transition, the behavior of such idealized pile-ups does not depart significantly from that of isolated elastic manifolds in random media, and stressed the fundamental difference with the behavior of three-dimensional assemblies of dislocations that exhibit metastable jammed configurations and avalanches even in the absence of quenched disorder.

Numerical models taking into account long-range interactions between multiple dislocations are in much better agreement with observations [2,13]. This suggests that these long-range interactions, instead of the short-range interactions between an elastic line and immobile obstacles, are at the root of the observed self-organized (essentially stress independent) critical plasticity. Here we focus on this transition from the behavior of a single dislocation interacting with obstacles to the collective dislocation dynamics, and analyze the motion of a small number of interacting dislocations across a field of fixed obstacles randomly distributed in their glide plane. The motion is thermally activated, i.e., the elastic manifold depinning problem is considered below the critical point.

A model previously employed to study the thermally activated motion of a single dislocation across fields of obstacles is used [14,15]. The model details are presented in these references. The dislocations are represented as flexible strings of line tension $\Gamma = 1/2Gb^2$ (G is the shear modulus and b is the Burgers vector length). Randomly distributed obstacles are placed in the glide plane. These may represent precipitates, solute clusters or other obstacles with which the dislocation interacts in the short range.

Under the action of the shear stress τ, a segment of length $l_c = 1/\sqrt{\rho}$ (ρ is the obstacle density) pinned by two obstacles bows out into an arc of dimensionless radius $r^* = 1/2\tau^*$. The applied shear stress τ^* is normalized by the Orowan stress Gb/l_c, $\tau^* = \frac{\tau l_c}{Gb}$. The force acting on the respective obstacles is $F = 2\Gamma \cos(\frac{\theta}{2})$, where θ is the angle made by the two branches of the dislocation impinging against the obstacle. Let us use the nondimensional form $f = \frac{F}{2\Gamma} = \cos(\frac{\theta}{2})$ for the force. The obstacle strength is defined as the maximum allowed force $f_c = \cos(\theta_c/2)$.

*Corresponding author; picuc@rpi.edu

The critical resolved shear stress τ_c^* at which dislocations glide through in absence of thermal activation is given by Friedel's result [16] $\tau_c^*=f_c^{3/2}$ (for randomly distributed obstacles). Here, the applied stress is normalized by the critical resolved shear stress: $\eta=\tau^*/\tau_c^*$. $\eta=1$ is a critical point for the system.

The obstacle-dislocation interaction is described in terms of an activation energy $\Delta G=2\Gamma d\Delta G^*$, where d is a characteristic interaction range. Γd becomes the unit of energy of the problem. The normalized activation energy is written $\Delta G^*=\Delta G_0^*(1-f^*)^n$, with $f^*=f/f_c$ being the reduced dislocation-obstacle interaction force. ΔG^* depends on the obstacle nature but decreases monotonically with f^*. The power $n=2$ is considered, which corresponds to obstacles with a triangular force-displacement profile.

The per-attempt probability that the dislocation overcomes an obstacle is given by the Arrhenius form $p=\exp(-\alpha\Delta G^*)$, where $\frac{1}{\alpha}=\frac{kT}{2\Gamma d}$ is the dimensionless temperature. The "circle rolling" procedure outlined in Ref. [17] is used to advance the dislocation. A stable configuration is obtained when two conditions are fulfilled at all obstacles in contact with the dislocation: the dislocation bows out into an arc of circle of radius smaller than the critical one (no Orowan looping) and the force acting on all obstacles is smaller than f_c.

Periodic boundary conditions are used in the direction parallel to the dislocation. The dimension of the model in this direction is important as spurious cutoffs in the distribution of jump areas may be introduced by these boundary conditions. We performed numerical studies varying the respective model size between $100l_c$ and $400l_c$ and concluded that as long as $\eta\leq 0.8$, the model size can be chosen $\sim 200l_c$. The model size in the direction of the dislocation motion is effectively infinite since the obstacle field is continuously renewed in front of the most advanced dislocation segment.

At low stress, a jump following release from an obstacle brings the dislocation to the next obstacle and the jump area S is on the order of l_c^2. This increases the probability of release at the pinning site immediately next to the released site along the current dislocation line and "unzipping" occurs. In this regime the activation energy for the entire dislocation glide process is equal to the activation energy for release at an individual obstacle (when all obstacles in the glide plane are identical) [14]. This mechanism is represented schematically in Fig. 1(a). The red dashed lines represent new equilibrium segments following thermally activated release.

At large resolved shear stress, the motion is jerky in the sense that upon release at an obstacle the dislocation bypasses multiple neighboring obstacles before finding a new equilibrium configuration [Fig. 1(b)]. In this regime the activation energy for dislocation motion is not identical to that for by-passing a single obstacle.

Single and multiple dislocations moving in the same glide plane across a field of randomly distributed identical obstacles are considered in this work. The dislocations interact through their stress field. Dislocation self-interaction (between segments of the same dislocation) is also considered. In order to apply the stress produced by the interaction of dislocation segments within the framework of the "circle rolling" procedure, the interaction stress is computed at the center point of each dislocation segment. This additional stress is applied as a constant field to the entire segment, which remains circular. This is an approximation since the stress field introduced by interactions is expected to vary along the representative dislocation. However, we conjecture that this approximation has limited effect on the overall dynamics.

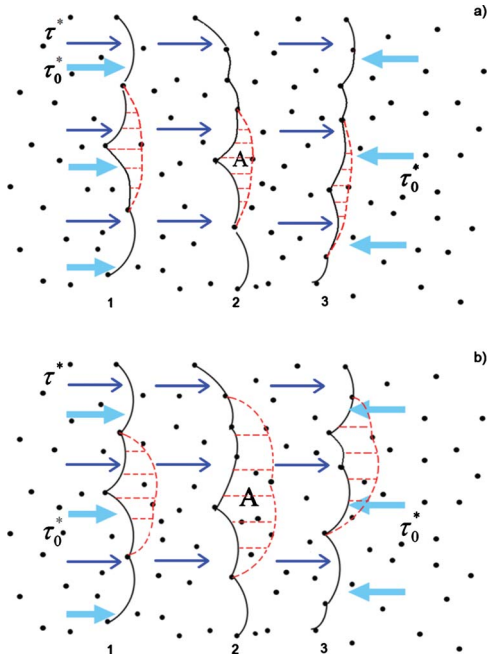

FIG. 1. (Color online) Schematic representation of a pack of three interacting dislocations performing (a) unzipping and (b) jerky motion. The red dashed lines represent equilibrium configurations after a release event at one pinning point of the previous stable configuration (continuous black lines). In the jerky mode the dislocation bypasses multiple obstacles. The arrows represent the confining stress τ_0^* acting on the outer dislocations in order to hold the pack together.

The dislocations in the pack are forced together by a constraining shear stress τ_0^* which is applied to the first and the last dislocations of the pack (Fig. 1). This constraining stress insures that the average distance between them remains constant in time. All dislocations are equally subjected to the far field applied stress. The results reported below for packs of dislocations (three and five dislocations) refer to the behavior of the middle dislocation of the pack. This way we analyze how the elastic interaction between dislocations modifies the jerky motion of individual dislocations. In this study we select τ_0^* equal to 10% of the far field stress τ^*. The average distance between dislocations in the pack is small enough (~ 8 to $10l_c$) to ensure significant elastic interaction between them.

Figures 2(a) and 2(b) show the distribution of jump areas, $P(S)$, for systems of a single dislocation (1d), and of three (3d), and five (5d) interacting dislocations subjected to stress in the unzipping range, $\eta=0.4$, and to $\eta=0.6$ and $\eta=0.8$ in the jerky range. Obstacles are weak, with obstacle strength $f_c=0.1$ in all simulations. The divergence of the cutoff size

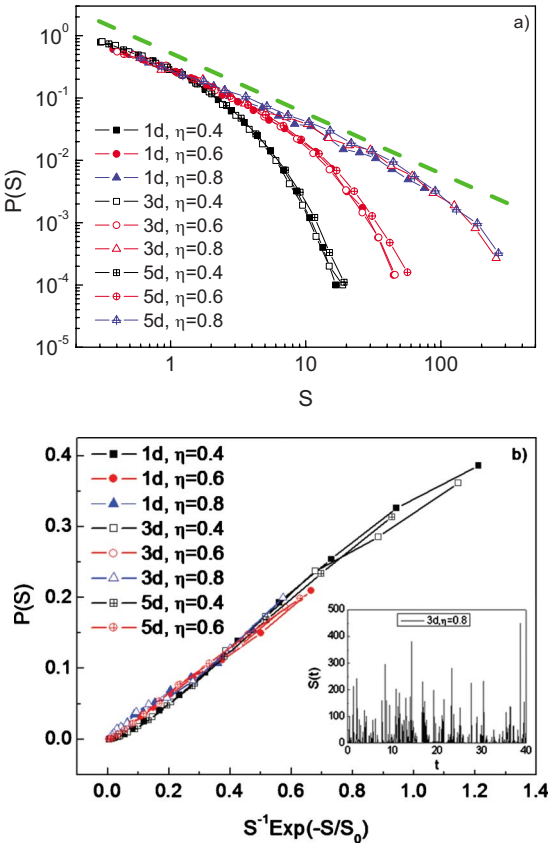

FIG. 2. (Color online) Probability density distribution functions of dislocation jump amplitudes for a single dislocation (1d) and for the central dislocation of packs of three (3d) and five (5d) dislocations. (a) curves showing the divergence of the cutoff size S_0 as the critical point $\eta=1$ is approached. The dashed line has slope −1. (b) master curve obtained by normalization with $S_0=1.03(1-\eta)^{-3.13}$, $S_0=1.07(1-\eta)^{-3.38}$ and $S_0=1.13(1-\eta)^{-3.47}$ for 1d, 3d, and 5d, respectively. The inset shows part of a recorded signal for the 3d system with $\eta=0.8$.

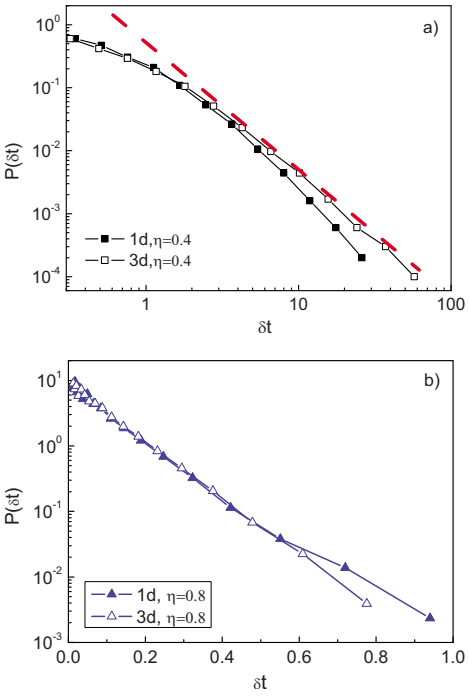

FIG. 3. (Color online) Probability distribution functions of wait times between unpinning events for a) $\eta=0.4$ (log-log plot) and (b) $\eta=0.8$ (semilog plot). The distribution is exponential at small δt and power law at large δt. The dashed line in (a) has slope −2.

S_0 as the applied stress increases toward the critical point $\eta=1$ is seen in Fig. 2(a). In this limit, the distribution function becomes a power law, $P(S)\sim S^{-\tau_S}$ with exponent $\tau_S\approx 1$. Dislocation-dislocation interaction (3d and 5d cases) does not change τ_S; in all instances, τ_S remains below the collective dislocation dynamics exponent, τ_A.

Signals collected from systems with multiple dislocations (3d and 5d) were used to generate a cumulative signal obtained by summing up jump amplitudes at given time (presumably closer to an AE measurement): $S^*(t)=\Sigma_i S_i(t)$, where $S_i(t)$ is the jump area of dislocation i of the pack. However, the corresponding distributions $P(S^*)$ essentially overlap $P(S)$.

The data is replotted in Fig. 2(b) as a master curve obtained by fitting the functional form $P(S)\sim S^{-\tau_S}\exp(-S/S_0)$ to the data in Fig. 2(a), with $\tau_S=1$ and $S_0\sim(1-\eta)^{-\chi}$. The exponent χ, which is related to the rate of divergence of the correlation length, is observed to increase with the number of dislocations in the pack: $\chi=3.13$, 3.38, and 3.47 for 1d, 3d, and 5d, respectively.

We computed the roughness exponent ζ by taking the Fourier transform of the dislocation line profile; the power spectrum of this function is expected to be a power function of exponent $-(2\zeta+1)$. At low η ($\eta=0.4$), the thermal exponent $\zeta=0.5$ results, while at higher η a transition is observed from an exponent $\zeta=0.8$ (close to the value of 2/3 reported previously) at large length scales, to $\zeta=0.5$ at small length scales. The transition moves to smaller length scales as η increases, such that for $\eta=0.6$ and 0.8, the larger $\zeta=0.8$ dominates. These roughness exponents and dependence on η were also obtained by Kolton *et al.* [18] for the Langevin dynamics of an elastic manifold. These authors also indicate [19] the existence of a roughness exponent $\zeta=1.26$ at very low temperatures. The roughness exponent does not change with the number of dislocations in the pack.

We consider next the intermittency of dislocation motion, and how it is modified by long-range interactions between dislocations. We analyze first the time series formed by the wait times between jumps, $\delta t(t)$. If the distribution of δt is Poissonian, the motion is random and the jumps are not clustered in time. Departures from this situation are observed in all data sets, with the mean of the distribution being smaller than the standard deviation; this is interpreted as an indication of intermittent dynamics.

Figures 3(a) and 3(b) represent the distribution functions $P(\delta t)$ for the 1d and 3d cases and for small and large applied stress, $\eta=0.4$ and $\eta=0.8$, respectively. The distribution is closer to an exponential in the low δt limit and appears to transform into a power law in the large δt limit, the transition being controlled by the applied stress. Dislocation-dislocation interaction leads to a better-defined power law tail and to increasing difference between the mean and standard deviation of the distribution, i.e., to more pronounced

intermittency. These observations are independent of the integration time step, which is chosen small enough to ensure at least several time steps per dislocation wait time. Actually, the curves are well approximated by $P(\delta t) \sim [(1-e^{-\delta t/b})/(\delta t/b)]^m$, with $(b,m)=(0.8,2.3)$, (0.3,4), and (0.2,5.2) for $\eta=0.4$, 0.6, and 0.8, respectively. This functional form has a power law tail $P(\delta t) \sim (\delta t/b)^{-m}$ for large δt, and is exponential, $P(\delta t) \sim e^{-m\delta t/2b}$, for small δt. The transition from the exponential to the power law-dominated range takes place at about $\delta t=2b$. The exponent m is seen to increase with η.

A more detailed study of intermittency in these signals can be performed by means of multifractal analysis, as previously used in turbulence [20] as well as to analyze jerky flow in alloys exhibiting Portevin–Le Chatelier effect [21] or AE signals obtained from deforming single crystals [6]. The time series S(t) was mapped to a signal with equally spaced samples. The jerk intensity at each such "grid point" was computed as $u_i=u(t_i)=\int_{t_i-\Delta t/2}^{t_i+\Delta t/2} S(t')dt'$, i.e., the sum of all dislocation jumps over the respective temporal bin of length Δt. The qth moment of the distribution function of series **u** was computed. These moments depend on Δt and the expected scaling is $Z_{\Delta t}(q)=\Sigma_i u_i^q \sim \Delta t^{(q-1)D(q)}$, where $D(q)$ is the generalized fractal dimension. The nonlinearity of the spectrum $D(q)$ is a signature of intermittency. The curves $Z_{\Delta t}$ versus Δt are power laws, provided the probing scale Δt is larger than the maximum wait time interval δt. Results of the analysis are shown in Fig. 4. The generalized fractal dimension $D(q)$ exhibits nonlinear variation with q in all cases. However, the curvature, i.e., the intermittent character of the motion, is more pronounced when approaching the critical point. Dislocations interaction also increases the intermittency (see inset of Fig. 4).

To probe the contribution of the signal amplitude and that of the waiting times to this effect, the signal S(t) was modified by replacing either the jump amplitude, S, or the wait time, δt, with random signals, while keeping the other measure unchanged. Randomizing the wait time series (while preserving the mean of the distribution constant) completely eliminates the intermittency, rendering $D(q)$ linear. Performing the opposite operation, randomizing the amplitudes while keeping the wait times unchanged, leads to little or no change in $D(q)$. Furthermore, the wait times and the amplitudes of the jumps are not correlated. Likewise, successive amplitude values are not correlated. This means that the area swept by the dislocation in a given event is essentially determined by the local obstacle distribution, which is random. These conclusions remain valid even when using cumulative jump amplitudes S^*.

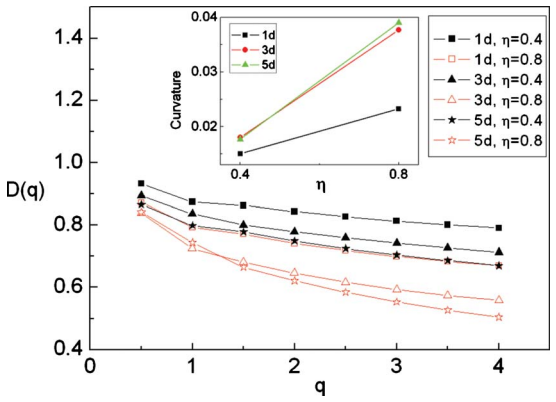

FIG. 4. (Color online) Multifractal analysis of $S(t)$ at low and high applied stress. The inset shows the curvature $\partial^2 D(q)/\partial q^2$ (evaluated numerically) of the curves in the main figure. The generalized fractal dimension D varies over the range studied. Dislocation-dislocation interaction as well as increasing the applied stress (η) increase the curvature of $D(q)$ indicating more pronounced intermittency.

In conclusion, field-mediated dislocation interaction promotes the appearance of intermittency and modifies the correlation length exponent, therefore appearing to lead to a transition from the less rich dynamics of a single dislocation to that of large ensembles of interacting dislocations as evidenced by AE experiments. However, long-range interactions between few dislocations does not solve the contradictions between the depinning problem and the collective dislocation dynamics discussed in introduction.

[1] M. Zaiser, Adv. Phys. **55**, 185 (2006).
[2] M. C. Miguel, A. Vespignani, S. Zapperi *et al.*, Nature (London) **410**, 667 (2001).
[3] J. Weiss and M.-C. Miguel, Mater. Sci. Eng., A **387**, 292 (2004).
[4] J. Weiss and D. Marsan, Science **299**, 89 (2003).
[5] J. Weiss and J. R. Grasso, J. Phys. Chem. B **101**, 6113 (1997).
[6] J. Weiss, T. Richeton, F. Louchet *et al.*, Phys. Rev. B **76**, 224110 (2007).
[7] D. M. Dimiduk, C. Woodward, R. LeSar *et al.*, Science **312**, 1188 (2006).
[8] M. Zaiser, Mater. Sci. Eng., A **309-310**, 304 (2001).
[9] S. Zapperi and M. Zaiser, Mater. Sci. Eng., A **309-310**, 348 (2001).
[10] B. Bakó, D. Weygand, M. Samaras, W. Hoffelner, and M. Zaiser, Phys. Rev. B **78**, 144104 (2008).
[11] D. S. Fisher, Phys. Rep. **301**, 113 (1998).
[12] P. Moretti, M. Carmen Miguel, M. Zaiser, and S. Zapperi, Phys. Rev. B **69**, 214103 (2004).
[13] F. Csikor, C. Motz, D. Weygand *et al.*, Science **318**, 251 (2007).
[14] Z. Xu and R. C. Picu, Phys. Rev. B **76**, 094112 (2007).
[15] R. C. Picu, R. Li, and Z. Xu, Mater. Sci. Eng., A **502**, 164 (2009).
[16] J. Friedel, *Dislocations* (Addison-Wesley, Reading, MA, 1967).
[17] A. J. E. Foreman and M. J. Makin, Philos. Mag. **14**, 911 (1966).
[18] A. B. Kolton, A. Rosso, and T. Giamarchi, Phys. Rev. Lett. **95**, 180604 (2005).
[19] A. B. Kolton, A. Rosso, T. Giamarchi, and W. Krauth, Phys. Rev. Lett. **97**, 057001 (2006).
[20] D. Schertzer and S. Lovejoy, J. Geophys. Res. **92**, 9693 (1987).
[21] M. A. Lebyodkin and T. A. Lebedkina, Phys. Rev. E **73**, 036114 (2006).